



### 33 **Abstract**

34 Orientation is a fundamental cognitive faculty, allowing the behaving self to link his/her current  
35 state to their internal representations of the external world. Once exclusively linked to  
36 knowledge of the current place and present time, in recent years, the concept of orientation has  
37 evolved to include processing of social, temporal, and abstract relations. Concordantly with the  
38 growing focus on orientation, spatial disorientation has been increasingly recognized as a  
39 hallmark symptom of Alzheimer's disease (AD). However, few studies have sought to explore  
40 disorientation along the AD continuum beyond the spatial domain.

41 51 participants along the AD continuum performed an orientation task in the spatial, temporal  
42 and social domains. Under functional magnetic resonance imaging (fMRI), participants  
43 determined which of two familiar places/events/people is geographically/ chronologically/  
44 socially closer to them, respectively. A series of analyses revealed disorientation along the AD-  
45 continuum to follow a three-way association between (1) orientation domain, (2) brain region,  
46 and (3) disease stage. Specifically, participants with MCI exhibited impaired spatio-temporal  
47 orientation and reduced task-evoked activity in temporoparietal regions, while participants with  
48 AD dementia exhibited impaired social orientation and reduced task-evoked activity in  
49 frontoparietal regions. Furthermore, these patterns of hypoactivation coincided with Default  
50 Mode Network (DMN) sub-networks, with spatio-temporal orientation activation overlapping  
51 DMN-C and social orientation with DMN-A. Finally, these patterns of disorientation-  
52 associated hypoactivations coincided with patterns of fluorodeoxyglucose (FDG)  
53 hypometabolism and cortical atrophy characteristic to AD-dementia.

54 Taken together, our results suggest that AD may constitute a disorder of orientation,  
55 characterized by a biphasic process as (1) early spatio-temporal and (2) late social  
56 disorientation, concurrently manifesting in task-evoked and neurodegenerative changes in  
57 temporoparietal and parieto-frontal brain networks, respectively. We propose that a profile of  
58 disorientation across multiple domains offers a unique window into the progression of AD.

## 59 **Introduction**

60 Orientation is a fundamental cognitive faculty, allowing the behaving self to link his/her current  
61 state to their internal representations of the external world (Berrios, 1982; Peer, Salomon,  
62 Goldberg, Blanke, & Arzy, 2015). Commonly, orientation is evaluated in the spatial, temporal  
63 and social domains, and as such it is recognized as the bedrock of the neurological clinical  
64 evaluation (Mahendran, Chua, Feng, Kua, & Preedy, 2015; Rapoport & Rapoport, 2015).  
65 Nonetheless, standard evaluations of orientation are limited to testing only the patient's  
66 knowledge about the present time, current location and personal identity, resulting in low  
67 sensitivity to early cognitive decline (Peters-founshtein et al., 2018).

68 In recent years, several lines of research (Coughlan, Laczó, Hort, Minihane, & Hornberger,  
69 2018; DeIpolyi, A. R., Rankin, K. P., Mucke, L., Miller, B. L., Gorno-Tempini, 2007; El Haj  
70 & Antoine, 2018; Kunz et al., 2015; Peters-Founshtein et al., 2018) have demonstrated that  
71 spatial orientation is potentially affected early on by AD pathology. One such study (Coughlan  
72 et al., 2019) used the Sea Hero Quest (SHQ) spatial navigation paradigm to compare young,  
73 cognitively intact, heterozygote carriers of Apolipoprotein E (APOE)- $\epsilon 4$  alleles ( $\epsilon 3/\epsilon 4$ ), a  
74 known risk-multiplier of AD to demographically-matched healthy homozygote ( $\epsilon 3/\epsilon 3$ )  
75 participants. Comparing the two groups as they perform several goal-oriented wayfinding tasks  
76 revealed significant disruptions in navigation performance in people at-risk for AD showing no  
77 clinically detectable cognitive deficits. However, orientation is not restricted to the spatial  
78 domain. It involves other domains such as the temporal and social ones (Du, Basyouni, &  
79 Parkinson, 2021; Parkinson, Liu, & Wheatley, 2014; Peer et al., 2015), that have been shown  
80 to be progressively impaired along the AD-continuum (Dafni-Merom, Peters-Founshtein,  
81 Kahana-Merhavi, & Arzy, 2019; Peters-Founshtein et al., 2018). Moreover, tests of orientation  
82 have been found to better discriminate between cognitively normal (CN) and mild cognitive  
83 impairment (MCI) participants (95% accuracy) when compared to standard neuropsychological  
84 evaluations (Addenbrooke's Cognitive Examination (ACE) – 71%, Mini Mental State

85 Examination (MMSE) – 70%) (Peters-Founshtein et al., 2018). This superiority may stem from  
86 a considerable overlap between the patterns of orientation-evoked brain activity and patterns of  
87 AD neurodegeneration (Peters-Founshtein et al., 2018).

88         Independently, the pattern of orientation-evoked brain activity was found to markedly  
89 overlap with the Default Mode Network (DMN) (Hayman & Arzy, 2021; Peer et al., 2015;  
90 Peters-Founshtein et al., 2018). The DMN is a network of interconnected brain regions, active  
91 when individuals engage in self-referential tasks such as autobiographical memory retrieval and  
92 future planning (Buckner, Andrews-Hanna, & Schacter, 2008). Furthermore, AD  
93 neuropathology (amyloid- $\beta$  (A $\beta$ ) and tau) has been shown to carry increased probability of  
94 spreading within rather than outside of the DMN (Adams, Maass, Harrison, Baker, & Jagust,  
95 2019; Buckner et al., 2005; Franzmeier, Dewenter, et al., 2020; Franzmeier, Neitzel, et al.,  
96 2020). Subsequent studies, re-evaluating DMN homogeneity, have suggested the DMN is  
97 comprised of partially dissociated components, each underlying different cognitive functions  
98 (Andrews-Hanna, Reidler, Sepulcre, Poulin, & Buckner, 2010; A. J. Barnett et al., 2020, 2021;  
99 D. A. Barnett, Arnold, Valenzuela, Brayne, & Schneider, 2014; Buckner & DiNicola, 2019).  
100 Taken together, the overlapping patterns of DMN connectivity and orientation in space, time,  
101 and person, imply a latent model of inter-related neuropathological and cognitive changes in  
102 AD (Buckner et al., 2005).

103         In the current comprehensive study, we aimed to evaluate the relations between (1)  
104 spatio-temporal and social disorientation, (2) DMN subnetworks and (3) neurodegeneration, in  
105 individuals along the AD continuum, using positron emission tomography (PET)-functional  
106 magnetic resonance imaging (fMRI). Considering the neuropsychological profile of AD-related  
107 cognitive decline (early spatio-temporal and later social decline), jointly with multiple studies  
108 suggesting a segregation between spatio-temporal and social processing in the brain, we  
109 hypothesized that spatio-temporal and social orientation would be differently affected along the  
110 AD-continuum. Hence, we set to test and characterize these differences in behavioral

111 performance and brain activity in the context of DMN topology and patterns of AD-related  
112 neurodegeneration.

## 113 **Methods**

### 114 **Participants**

115 Fifty-one individuals (27 females, mean age  $71.43 \pm 0.82$ , for detailed demographics see Table  
116 1) participated in the study, including 35 cognitively impaired participants (12 with AD  
117 dementia and 23 with amnesic MCI) and 16 age-matched CN older adults. Participants  
118 underwent a complete neurological examination, cerebrovascular risk-factor assessment using  
119 the Hachinski Ischemic Scale (Hachinski et al., 1975), and a comprehensive  
120 neuropsychological evaluation that included the Clinical Dementia Rating (Morris, 1993),  
121 Montreal Cognitive Assessment (Nasreddine et al., 2005), ACE (Mathuranath, Nestor, Berrios,  
122 Rakowicz, & Hodges, 2000), and Frontal Assessment Battery (Dubois, Slachevsky, Litvan, &  
123 Pillon, 2000). Cognitively impaired participants met the National Institute on Aging and the  
124 Alzheimer's Association clinical criteria for AD-dementia or amnesic-MCI (Albert et al., 2011;  
125 S. Gauthier et al., 2006; Mckhann et al., n.d.; Petersen et al., 1999). All participants underwent  
126 structural T1 and T2 weighted MRI and fluorodeoxyglucose (FDG)-PET, which were reviewed  
127 by neuroradiology and nuclear medicine specialists to exclude non-AD etiologies. All  
128 participants provided written informed consent prior to undergoing study procedures, and the  
129 study was approved by the ethics committee of the Assuta Medical Center.

### 130 **Experimental stimuli**

131 Stimuli used in the task consisted of personally familiar names of places, events and people. To  
132 minimize the effects of memory disruptions on orientation testing, a set of personally familiar  
133 stimuli was obtained from each participant prior to testing. Participants were presented with a  
134 list of potential stimuli and for each were asked to approximate its location (for space stimuli)  
135 or year (for time stimuli). Failing to reference both the relevant region of the country and at  
136 least one nearby landmark (space) or miscalculating the correct year (time), resulted in the

137 removal of the specific stimulus from further testing. In addition, participants were asked to  
138 generate a list of 8 close family members, 8 friends, and 8 acquaintances, which was  
139 corroborated with either a child or spouse (for additional details see supplementary materials).

#### 140 **Experimental procedure - fMRI task**

141 In the orientation task, participants were presented with pairs of familiar stimuli consisting of  
142 names of either two cities in Israel, two events, or two people, and were asked to determine  
143 which of the two is closer to them: geographically closer to their current location for cities,  
144 chronologically closer to the present time for events, or personally closer to them for people.  
145 To standardize experimental sessions based on personalized sets of stimuli, stimuli were split  
146 into three distance categories. Trials were generated by pairing stimuli from adjacent distance  
147 categories only. Stimuli were presented using the Presentation software (Version 18.0,  
148 Neurobehavioral Systems, Inc., Berkeley, CA; for additional details see supplementary  
149 materials).

150 Trials were presented in a randomized block design, with each block containing three  
151 consecutive trials belonging to a specific domain and distance category. Each trial was  
152 presented for a maximum of 10 seconds (5 TRs). Experiments consisted of four experimental  
153 runs, each containing 12 three-trial blocks in randomized order, balanced for both domain and  
154 distance categories. Additionally, participants performed a lexical control task in two additional  
155 separate runs. In the lexical control task, participants were presented with stimuli pairs from the  
156 same sets but were instructed to indicate which of the words contains the letter “A”. Stimuli  
157 were presented using the Presentation software (Version 18.0, Neurobehavioral Systems, Inc.,  
158 Berkeley, CA). Prior to the experiment, A 5-minute training task containing different stimuli  
159 was administered. See supplementary materials for more details. The task was modeled on our  
160 previous studies of orientation (Dafni-Merom et al., 2019; Hayman & Arzy, 2021; Peer et al.,  
161 2015; Peters-Founshtein et al., 2018)

#### 162 **Statistical analyses**

163 Efficacy scores (ES) (Townsend & Ashby, 1983) were computed for each participant and  
164 domain separately by calculating the ratio between the success rate (SR) and mean response  
165 time (RT). A global ES was calculated for each participant by averaging the ESs across the  
166 three domains. Subsequently, mean ESs were compared across the three groups (AD dementia,  
167 MCI, CN) using analysis of variance (ANOVA) and Tukey-Kramer post-hoc tests. For the  
168 neuropsychological tests, scores were recorded according to the relevant testing guidelines.

### 169 **MRI and PET Data Acquisition and Preprocessing**

170 For details regarding MRI and FDG-PET data acquisition and preprocessing please refer to  
171 supplementary materials.

#### 172 **Voxel-based morphometry (VBM)**

173 We applied voxel-based morphometry (VBM) analysis to compare gray matter (GM) density  
174 between CN, MCI and AD dementia groups (Ashburner & Friston, 2000). Specifically, we  
175 used a general linear model (GLM) (Worsley & Friston, 1995) to perform voxel-wise two-  
176 sample t-test for each of the clinical contrasts (CN–MCI, MCI–AD-dementia, CN–AD-  
177 dementia), with age, years of education, gender and total intracranial volume included as  
178 nuisance variables (see Supplementary Figure S1). Here, and in all further analyses we applied  
179 a false discovery rate (FDR) correction for multiple comparisons ( $P < 0.05$ ), and cluster size  
180 thresholding of 20 voxels. All analyses were performed using the statistical parametric mapping  
181 (SPM) 12 software package (version 7219), and in-house Matlab scripts (version 2019b,  
182 Mathworks, Natick, MA, USA). In-house scripts are publicly available  
183 (<https://www.neuropsychiatrylab.com/codes>).

#### 184 **PET Analysis**

185 To correct for AD-unrelated variance, FDG standardized uptake values (SUV) were first  
186 normalized by mean cerebellar GM SUV, to produce SUV ratio (SUVr) maps (Marcus, Mena,  
187 & Subramaniam, 2014). We then constructed a GLM to compare glucose uptake between the  
188 CN, MCI and AD dementia groups. Specifically, we performed voxel-wise two-sample t-tests

189 comparing SUVR values between the three clinical contrasts (CN–MCI, MCI–AD-dementia,  
190 CN–AD-dementia), with age, years of education, and gender included as nuisance variables  
191 (Figure S1) (Kanda et al., 2008).

## 192 **Identification of orientation-evoked activity**

193 To assess the selective activations elicited by different experimental conditions, we applied a  
194 group-level random-effects GLM analysis using data from all participants. To isolate  
195 orientation-specific activity, we contrasted the (1) spatial and temporal conditions (spatio-  
196 temporal) and, separately, the (2) social condition with the lexical control task (Peer et al.,  
197 2015).

## 198 **Orientation task analysis**

199 We used a group-level random-effects GLM to compare spatio-temporal and social evoked  
200 activations between the CN, MCI, and AD dementia groups. Specifically, we performed voxel-  
201 wise two-sample t-tests comparing task parameter estimates of each domain in the three clinical  
202 contrasts with age, years of education, and gender included as nuisance variables. To exclude  
203 non-specific activations, maps of task over lexical control in all participants served as inclusive  
204 masks.

## 205 **Region-of-interest analysis**

206 To associate task-evoked patterns of brain activity as well as glucose metabolism in the brain  
207 to DMN topology, ROIs for DMN subnetworks A, B, and C were extracted from the Schaefer  
208 200 atlas (Schaefer et al., 2018). DMN ROIs were used to compare GM density, glucose uptake  
209 (Figure S2), and task evoked activity (parameter estimates of space-time and person over rest)  
210 between CN, MCI, and AD dementia groups. ANOVA and the Tukey-Kramer post-hoc test  
211 were used in all the comparisons.

## 212 **Mediation analysis**

213 We set to test the hypothesis that neurodegeneration, expressed as changes in glucose  
214 metabolism, accounts for some of the shared variance between orientation-evoked activity and



215 orientation performance along the AD continuum. For this purpose, we conducted a whole-  
216 brain voxel-wise mediation analysis using the Bootstrap Regression Analysis of Voxelwise  
217 Observations (BRAVO) toolbox (<https://sites.google.com/site/bravotoolbox>). Two three-path  
218 models were constructed, separately for spatio-temporal and social tasks (see Figure 4A), with  
219 parameter estimates for task-over-rest as the predictor variable (“X” in Figure 4A), task ES as  
220 outcome variable (“Y” in Figure 4A), and FDG-SUVr as mediator variable (“M” in Figure 4A).  
221 The mediation analysis tested whether the relation (path c) between the predictor variable (“X”,  
222 space-time/person beta) and an outcome variable (“Y”, space-time/person ES) is significantly  
223 attenuated when the relation between X and a mediator variable (“M”, FDG-SUVr) (path a)  
224 and the relation between M and Y (path b) are added to the model (Figure 4A). Mediation effect  
225 sizes were computed for every voxel. Significance was assessed through a permutation  
226 procedure with 10,000 iterations and corrected through FDR for voxel-wise multiple  
227 comparisons. Importantly, Models were applied to all participants and were agnostic to the  
228 clinical labels. To test the specificity of the mediation-related effects for the orientation tasks,  
229 we repeated the above analysis for the space-time and person domains of the lexical control  
230 task (Figure S3).

### 231 **Permutation analysis for overlap significance**

232 We performed overlap analysis to assess the correspondences between DMN-A, B, and C ROIs;  
233 spatio-temporal and social orientation-evoked maps of activity (Figure 3); spatio-temporal and  
234 social maps of mediation (Figure 4); and clinical contrasts for VBM (Figure S1) and FDG-  
235 SUVr (Figure S1). To assess overlap we quantified the shared number of suprathreshold  
236 (orientation, mediation, VBM, FDG) and DMN ROI voxels and divided by the total number of  
237 DMN ROI voxels. To determine significance of overlap we used a permutation analysis. We  
238 generated 10,000 permutation maps in which the same number of suprathreshold voxels was  
239 randomly shuffled, and then calculated the proportion of permutation maps in which the shared  
240 number of voxels was equal to or greater than the overlap between the original masks. This

241 effectively determined the probability of observing the level of overlap we found with a random  
242 pattern of suprathreshold parameter.

## 243 **Results**

### 244 **Spatio-temporal and social orientation performance is differently affected along the AD-** 245 **continuum**

246 Behavioral results for the orientation task across all domains showed significant differences  
247 between the 3 clinical groups ( $p < 0.05$ , ANOVA and Tukey-Kramer post-hoc test). Participants  
248 with AD-dementia scored significantly lower than participants with MCI, and the latter— lower  
249 than CN participants (mean $\pm$ SEM:  $0.17 \pm 0.02$ [ $sec^{-1}$ ],  $0.32 \pm 0.021$ [ $sec^{-1}$ ],  $0.41 \pm 0.02$ [ $sec^{-1}$ ];  
250 Figure 1A). Efficacy scores (ES) in the spatio-temporal domains (mean $\pm$ SEM:  $0.15 \pm 0.02$ [ $sec^{-1}$ ]  
251  $^1$ ],  $0.29 \pm 0.02$ [ $sec^{-1}$ ],  $0.38 \pm 0.02$ [ $sec^{-1}$ ]; Figure 1B) showed significant differences between all 3  
252 clinical groups (AD dementia, MCI, CN, respectively;  $P < 0.05$ ). ES in the social domain  
253 (mean $\pm$ SEM:  $0.21 \pm 0.03$ [ $sec^{-1}$ ],  $0.42 \pm 0.02$ [ $sec^{-1}$ ],  $0.48 \pm 0.02$ [ $sec^{-1}$ ]; Figure 1C) showed  
254 significant differences only between AD-dementia and non-AD participants (CN and MCI),  
255 comparable with the lexical control task (mean $\pm$ SEM:  $0.4 \pm 0.07$ [ $sec^{-1}$ ],  $0.68 \pm 0.04$ [ $sec^{-1}$ ],  
256  $0.82 \pm 0.06$  [ $sec^{-1}$ ]; Fig. 1D).

### 257 **Divergent changes in spatio-temporal and social activity along the AD continuum:**

258 Spatio-temporal orientation was shown to activate the precuneus, parieto-occipital sulcus,  
259 anterior and posterior cingulate cortices, parahippocampal and supramarginal gyri bilaterally,  
260 and the left superior frontal gyrus (Figure 2A). Social orientation activated the anterior and  
261 posterior cingulate cortices, and the angular and the superior medial gyri, and the putamen  
262 bilaterally (Figure 2A). Subsequent second level GLM analysis revealed significant differences  
263 in spatio-temporal orientation between CN and MCI participants and CN and AD-dementia  
264 participants in the precuneus, posterior cingulate cortex, parahippocampal gyri and  
265 hippocampus bilaterally (Figure 2B). Second level GLM analysis of social orientation showed

266 significant differences between MCI and AD-dementia participants as well as CN and AD-  
267 dementia participants in the precuneus, superior medial and angular gyri bilaterally (Figure 2C).

268 **Spatio-temporal and social orientation-evoked activity overlap differently with Default**  
269 **Mode sub-networks.**

270 To examine whether discrete brain networks underlie spatio-temporal and social orientation we  
271 overlapped suprathreshold task-evoked activation maps with DMN A, B, and C ROIs. Spatio-  
272 temporal orientation activity was found to significantly overlap the DMN-C (27%,  $P < 0.001$ ,  
273 Figure 3A and B). Social orientation activations were found to significantly overlap the DMN-  
274 A (28%,  $P < 0.001$ ), and B (11%,  $P < 0.001$ , 3A and B). We then compared mean task evoked  
275 coefficient estimated for spatio-temporal and social orientation among the CN, MCI and AD  
276 dementia groups, in each of the DMN ROIs. DMN ROI analysis for the spatio-temporal  
277 orientation showed differences between CN and MCI and AD-dementia participants in DMN-  
278 C only ( $P < 0.05$ , Figure 3C and S2A). For social orientation, DMN ROI analysis showed  
279 differences between AD-dementia participants and MCI and CN participants in DMN A and B  
280 only ( $P < 0.05$ , Figure 3C and S2B).

281 **AD-related hypometabolism mediates the relations between orientation performance and**  
282 **orientation-evoked activity**

283 Spatio-temporal mediation effects were found to be significant ( $P < 0.05$ , FDR-corrected) in the  
284 parahippocampal gyrus, posterior cingulate cortex and precuneus, significantly overlapping  
285 DMN-A (7%,  $P < 0.001$ , Figure 4C) and DMN-C (17%,  $P < 0.001$ , Figure 4C). Social mediation  
286 effects were found to be significant in the precuneus ( $P < 0.05$ , FDR-corrected), significantly  
287 overlapping with DMN-A (7%,  $P < 0.001$ , Figure 4C) and DMN-C (8%,  $P < 0.001$ , Figure 4C).  
288 Mediation analysis for the lexical control task in space-time revealed small overlap with DMN-  
289 C (1%,  $P < 0.001$ , Figure S3B and C). Social lexical mediation analysis revealed small overlap  
290 with DMN A (3%,  $P < 0.001$ , Figure S3B2 and S3C2).

291 **Discussion**

292 Our study revealed that an early stage of AD-related decline, MCI, manifests in spatio-temporal  
293 disorientation and task-evoked hypoactivation in temporoparietal regions, significantly  
294 overlapping the DMN-C subnetwork. Participants at the later stage of AD-dementia exhibited  
295 social disorientation and task-evoked hypoactivation in frontoparietal regions, significantly  
296 overlapping the DMN-A subnetwork. Moreover, the changes in task-evoked brain activity  
297 followed the pattern of glucose hypometabolism. Mediation analysis showed hypometabolism  
298 to mediate the relations between orientation-evoked activity and task performance along the  
299 AD continuum.

300 The DMN is a network of interconnected brain regions, which includes medial prefrontal,  
301 posterior cingulate and hippocampal brain structures. The DMN is known to activate when  
302 individuals engage in self-referential tasks, such as autobiographical memory retrieval and  
303 future planning (Buckner et al., 2008). In AD, early works have demonstrated a high degree of  
304 overlap between maps of DMN connectivity and patterns of structural and metabolic  
305 disruptions, as well as A $\beta$  and tau deposition (Buckner et al., 2005; Hoenig et al., 2018;  
306 Palmqvist et al., 2017). More specifically, in AD patients, functionally connected regions were  
307 found to correlate with tau accumulation rates (Franzmeier, Neitzel, et al., 2020), corroborating  
308 the hypothesis that DMN connectivity facilitates trans-synaptic dispersion of tau across the  
309 brain (Adams et al., 2019; Buckner et al., 2005; Franzmeier, Dewenter, et al., 2020; Franzmeier,  
310 Neitzel, et al., 2020). Independently, several works have shown the DMN to comprise several  
311 distinct subnetworks (Andrews-Hanna et al., 2010; Buckner et al., 2008; Buckner & DiNicola,  
312 2019). The detailed organization of these networks is revealed both in group and single subject  
313 level analyses. Evidence emerging from such studies suggests that the DMN comprises two or  
314 three separate networks with clear spatial distinctions along the posterior and anterior midline.  
315 Here we demonstrated the association between DMN subnetworks and spatio-temporal and  
316 social orientation in AD. Specifically, our findings suggest that disorientation, manifesting as

317 progressive disruptions in behavioral performance and task-evoked brain activity is linked to  
318 sequential disruption in DMN-C (early) and DMN-A (late) regions along the AD continuum.  
319 Jointly, these results raise the possibility that DMN subnetworks are associated with distinct  
320 phases in AD progression.

321 Additional sources of evidence offer complementary accounts of the roles DMN subnetworks  
322 potentially play in AD pathology. PET neuroimaging of the two molecular AD hallmarks, A $\beta$   
323 and tau, has revealed distinct patterns of deposition across the brain. A $\beta$  initially accumulates  
324 in medial parietal regions and spreads from neocortex to allocortex to brainstem. Tau, by  
325 contrast, first becomes evident in the entorhinal cortex, from which it spreads to limbic areas,  
326 and from there to the neocortex. In early stages of the disease, the pattern of A $\beta$  deposition  
327 markedly overlaps with DMN A, while tau deposition markedly overlaps with DMN-C (van  
328 der Kant, Goldstein, & Ossenkoppele, 2020). Jointly, the associations between A $\beta$ , tau and  
329 DMN subnetworks and our findings showing early DMN-C and late DMN-A hypometabolism,  
330 may suggest that at later stages of the disease, A $\beta$  accumulation in DMN A facilitates the spread  
331 of tau beyond DMN C brain regions (Busche & Hyman, 2020). As A $\beta$  was independently  
332 shown to affect functional connectivity (Lin et al., 2020), it is possible that A $\beta$  facilitates tau  
333 spread beyond DMN-C regions by altering DMN A/C connectivity. This hypothesis is  
334 supported by the discovery of primary age-related tauopathy (PART), a neuropathological  
335 entity defined by the presence of tau in the absence of A $\beta$ , which has been characterized by (1)  
336 tau remaining confined to the MTL regions and (2) appearing in cognitively intact older adults  
337 (Crary et al., 2014). As the nature of the relationship between A $\beta$  and tau eludes consensus, the  
338 prospect of functional connectivity, specifically between subnetworks of the DMN, could  
339 potentially inform the mechanisms of propagation of AD neuropathology across the brain.

340 Our findings not only mark the significance of orientation testing in AD but also may suggest  
341 a role for AD as a potential neurodegenerative disease model of disorientation (Peer, Lyon, &  
342 Arzy, 2014). From this perspective, our results may contribute to the enduring question of

343 domain-specific (B. Gauthier & van Wassenhove, 2016; Silson, Steel, Kidder, Gilmore, &  
344 Baker, 2019) versus domain-general (Park, Miller, & Boorman, 2021) systems of orientation.  
345 Coinciding with previously published findings (Kumaran & Maguire, 2005; Peer et al., 2015;  
346 Silson et al., 2019), here we linked spatio-temporal and social processing with temporoparietal,  
347 and frontoparietal regions, respectively. The diverging patterns of activity and vulnerability  
348 along the AD continuum for spatio-temporal and social orientation suggests a domain-dedicated  
349 framework, with its various components sequentially affected along the AD continuum.

350         However, several studies have challenged this paradigm of spatio-temporal and social  
351 dedicated brain regions, showing that, under some conditions, temporoparietal regions are  
352 involved in social-domain tasks, and frontoparietal regions - with spatial tasks. As a possible  
353 way of reconciling these seemingly contradictory findings, we propose that spatio-temporal and  
354 social activations represent special cases of archetypical modes of information processing  
355 (Kaplan & Friston, 2018; Peer et al., 2014; Whittington, McCaffary, Bakermans, & Behrens,  
356 2022), underlied by temporoparietal (DMN-C) and frontoparietal (DMN-A) regions,  
357 respectively (Byrne, Becker, & Burgess, 2007; Whittington et al., 2020). Specifically, DMN-C  
358 regions were proposed to prioritize relational information, while DMN-A regions were found  
359 to accentuate self-referential aspects of the experience. In our task, relational and self-  
360 referential processes associated with spatio-temporal and social orientation, respectively,  
361 however under different task conditions these associations could potentially shift. In future  
362 studies we intend to generalize beyond specific tasks and define the underlying cognitive roles  
363 of the DMN subnetworks.

364 Social engagement in AD has been explored from several perspectives (Bennett, Schneider,  
365 Tang, Arnold, & Wilson, 2006; Fredericks et al., 2018; Sabat & Gladstone, 2010; Sabat & Lee,  
366 2012; Sturm et al., 2013; Wilson et al., 2007). One approach focuses on disruptions in social  
367 mapping and orientation, i.e the ability to mentalize relational representation of other people  
368 within a multi-dimensional (social) space (Schafer & Schiller, 2018). Here we demonstrate the

369 relative resilience of social orientation, which finally breaks down in the later stages of AD,  
370 and its association to the DMN-A subnetwork. Brain systems, such as hippocampal place cells  
371 or entorhinal grid cells, once considered dedicated to spatial computations, are gradually  
372 recognized for their role in social cognition (Omer, Maimon, Las, & Ulanovsky, 2018; Park et  
373 al., 2021). In an aforementioned study, Tavares and colleagues have shown that hippocampal  
374 BOLD signal during social “navigation” in the dimensions of power and affiliation was  
375 negatively correlated with social avoidance and neuroticism, suggesting a link between social  
376 orientation and interpersonal traits. Here we present evidence suggesting that a relative  
377 preservation of social orientation in early stages of AD (followed by late disruption) is linked  
378 to relatively late neurodegeneration in the DMN-A subnetwork regions. In the context of studies  
379 mapping social orientation to MTL structures, our results suggest that in addition to previously  
380 reported MTL regions, frontoparietal DMN-A regions play a critical role in social orientation.

381 To the best of our knowledge, ours is the first study to utilize a combination of PET  
382 and MR imaging to simultaneously assess neurodegeneration, task-induced brain activity, and  
383 performance within a single cohort. We used mediation analysis to jointly analyze functional,  
384 metabolic, and behavioral data, to examine whether (and where in the brain) hypometabolism  
385 mediates the relationship between orientation-evoked activity and task performance along the  
386 AD continuum. We conducted mediation analyses separately for spatio-temporal and social  
387 orientation, as well as for a lexical control task, matching the orientation task in format and  
388 stimuli yet differing in its cognitive requirements. For spatio-temporal and social orientation,  
389 mediation effects were found to be significant in DMN C and DMN A medial regions,  
390 respectively, suggesting AD-related neurodegeneration induces changes beyond simply  
391 suppressing activity and disrupting performance, but rather affecting the relations between  
392 activity and performance (Huijbers et al., 2015). Additional studies have shown mixed patterns  
393 of hypo- and hyperactivation in patients along the AD spectrum (Foster, Kennedy, Horn,  
394 Hoagey, & Rodrigue, 2018; R. Sperling, 2007). In one such study, Kunz and colleagues (Kunz

395 et al., 2015) demonstrated that young asymptomatic APOE- $\epsilon$ 4 carriers (AD risk multiplier)  
396 exhibit decreased entorhinal and increased hippocampal activity while navigating a 3D arena.  
397 Exploring later, clinically detectable, stages of AD, O'Brien and colleagues (O'Brien et al.,  
398 2010) administered a memory-encoding task to a group of MCI and older adult control  
399 participants while undergoing fMRI. The results demonstrated that while both groups were  
400 similarly successful in recall, stronger hippocampal activation in the MCI group during  
401 encoding correlated to a higher rate of cognitive decline, and sequential hypoactivation in  
402 follow-up scans. The effects of AD on brain activity therefore appear to relate both to the stage  
403 of the disease and to the task itself. In future efforts, we intend to model relationships between  
404 brain activity and behavior with specific neuroimaging markers of AD-pathology.

405 Our results and conclusion notwithstanding, this work is not free from limitations. First, in  
406 recent years there has been a push for progressively shifting the definition of AD from a  
407 syndromal to a biological one (Jack et al., 2018). Specifically, AD biomarkers, including A $\beta$ ,  
408 tau and neurodegeneration have been reorganized into the ATN framework (Kern et al., 2018).  
409 In the current study we focused on 2 separate markers of neurodegeneration: structural MRI  
410 and FDG-PET. In future studies we intend to incorporate A $\beta$  and tau PET imaging in order to  
411 shift the focus from networks and activity to pathology. Additionally, the current study was  
412 cross-sectional and had a relatively small sample size, especially when considering the  
413 inclusion of 3 diagnostic groups (CN, MCI, and AD dementia). Future studies will consist of  
414 larger sample sizes and longitudinal follow-up, allowing us to better understand the  
415 directionality of these brain-behavior associations and their evolution over time in AD.

416 In conclusion, this study demonstrates the central role of disorientation in AD, and specifically  
417 the potential of evaluating orientation in multiple domains to differentiate between disease  
418 stages. We suggest that the relative early vulnerability of spatial and temporal orientation  
419 (compared to social orientation) stems from its association with temporoparietal regions, which  
420 are affected in early stages of the disease. Comparably, the relative resilience of social



421 orientation stems from its association with the frontoparietal cortex, which is affected only in  
422 later stages of the disease. We attribute these associations to distinct underlying computations  
423 performed by functionally distinct subnetworks of the DMN. We suggest that in parallel with  
424 the rapidly evolving evidence in support of usage of biomarkers in AD diagnosis, establishing  
425 a data-driven neurocognitive profile of AD degeneration will greatly benefit disease diagnosis,  
426 monitoring and evaluation of treatment response.

427

#### 428 **Acknowledgements**

429 We are grateful to Zohar Nitsan, Inbal Machcat and Hagai Baruch for their help in participant  
430 scanning, and to Dr. Limor Shaharabani-Gargir for her invaluable help with participant  
431 management. To Dr. Michael Peer, Dr. Moshe Roseman and Mr. Amnon Dafni-Merom for  
432 their insightful comments. This work was supported by the Israeli Science foundation (grant  
433 no. 3213/19) and the NIH (grant no. R21 AG070877 to GAM, HS and SA). SA is grateful to  
434 Mr. Ronald Abramson and The Glazer foundation for their generous support.

435

436

437

438

439

440

441

442

443

444

445

446

447 **References**

- 448 Adams, J. N., Maass, A., Harrison, T. M., Baker, S. L., & Jagust, W. J. (2019). Cortical tau  
449 deposition follows patterns of entorhinal functional connectivity in aging. *ELife*, 8, 1–  
450 22. <https://doi.org/10.7554/eLife.49132>
- 451 Albert, M. S., DeKosky, S. T., Dickson, D., Dubois, B., Feldman, H. H., Fox, N. C., ...  
452 Phelps, C. H. (2011). The diagnosis of mild cognitive impairment due to Alzheimer's  
453 disease: Recommendations from the National Institute on Aging-Alzheimer's  
454 Association workgroups on diagnostic guidelines for Alzheimer's disease. *Alzheimer's*  
455 *and Dementia*, 7(3), 270–279. <https://doi.org/10.1016/j.jalz.2011.03.008>
- 456 Andrews-Hanna, J. R., Reidler, J. S., Sepulcre, J., Poulin, R., & Buckner, R. L. (2010).  
457 Functional-Anatomic Fractionation of the Brain's Default Network. *Neuron*, 65(4), 550–  
458 562. <https://doi.org/10.1016/j.neuron.2010.02.005>
- 459 Ashburner, J., & Friston, K. J. (2000). Voxel-based morphometry - The methods.  
460 *NeuroImage*, 11(6 I), 805–821. <https://doi.org/10.1006/nimg.2000.0582>
- 461 Barnett, A. J., Reilly, W., Dimsdale-Zucker, H., Mizrak, E., Reagh, Z., & Ranganath, C.  
462 (2020). Organization of cortico-hippocampal networks in the human brain. In *bioRxiv*.  
463 <https://doi.org/10.1101/2020.06.09.142166>
- 464 Barnett, A. J., Reilly, W., Dimsdale-Zucker, H. R., Mizrak, E., Reagh, Z., & Ranganath, C.  
465 (2021). Intrinsic connectivity reveals functionally distinct cortico-hippocampal networks  
466 in the human brain. In *PLoS Biology* (Vol. 19).  
467 <https://doi.org/10.1371/journal.pbio.3001275>
- 468 Barnett, D. A., Arnold, S. E., Valenzuela, M. J., Brayne, C., & Schneider, J. A. (2014).  
469 Cognition in Late Life. *Acta Neuropathol.*, 127(1), 137–150.  
470 <https://doi.org/10.1007/s00401-013-1226-2>.Cognitive
- 471 Bennett, D. A., Schneider, J. A., Tang, Y., Arnold, S. E., & Wilson, R. S. (2006). The effect  
472 of social networks on the relation between Alzheimer's disease pathology and level of

- 473 cognitive function in old people: a longitudinal cohort study. *Lancet Neurology*, 5(5),  
474 406–412. [https://doi.org/10.1016/S1474-4422\(06\)70417-3](https://doi.org/10.1016/S1474-4422(06)70417-3)
- 475 Berrios, G. E. (1982). Disorientation states and psychiatry. *Comprehensive Psychiatry*, 23(5),  
476 479–491. [https://doi.org/10.1016/0010-440X\(82\)90161-4](https://doi.org/10.1016/0010-440X(82)90161-4)
- 477 Buckner, R. L., Andrews-Hanna, J. R., & Schacter, D. L. (2008). The brain's default network:  
478 Anatomy, function, and relevance to disease. *Annals of the New York Academy of*  
479 *Sciences*, 1124, 1–38. <https://doi.org/10.1196/annals.1440.011>
- 480 Buckner, R. L., & DiNicola, L. M. (2019). The brain's default network: updated anatomy,  
481 physiology and evolving insights. *Nature Reviews Neuroscience*, 20(10), 593–608.  
482 <https://doi.org/10.1038/s41583-019-0212-7>
- 483 Buckner, R. L., Snyder, A. Z., Shannon, B. J., Larossa, G., Sachs, R., Fotenos, A. F., ...  
484 Mintun, M. A. (2005). Molecular, Structural, and Functional Characterization of  
485 Alzheimer's Disease: Evidence for a Relationship between Default Activity, Amyloid,  
486 and Memory. *Neuroscience*, 25(34), 7709–7717.  
487 <https://doi.org/10.1523/JNEUROSCI.2177-05.2005>
- 488 Busche, M. A., & Hyman, B. T. (2020). Synergy between amyloid- $\beta$  and tau in Alzheimer's  
489 disease. *Nature Neuroscience*, 23(10), 1183–1193. [https://doi.org/10.1038/s41593-020-](https://doi.org/10.1038/s41593-020-0687-6)  
490 [0687-6](https://doi.org/10.1038/s41593-020-0687-6)
- 491 Byrne, P., Becker, S., & Burgess, N. (2007). Remembering the past and imagining the future:  
492 a neural model of spatial memory and imagery. *Psychological Review*, 114(2), 340–375.  
493 <https://doi.org/10.1037/0033-295X.114.2.340>
- 494 Calhoun, V. D., & Sui, J. (2016). Multimodal Fusion of Brain Imaging Data: A Key to  
495 Finding the Missing Link(s) in Complex Mental Illness. *Biological Psychiatry:*  
496 *Cognitive Neuroscience and Neuroimaging*, 1(3), 230–244.  
497 <https://doi.org/10.1016/j.bpsc.2015.12.005>
- 498 Coughlan, G., Coutrot, A., Khondoker, M., Minihane, A. M., Spiers, H., & Hornberger, M.

- 499 (2019). Toward personalized cognitive diagnostics of at-genetic-risk Alzheimer's  
500 disease. *Proceedings of the National Academy of Sciences of the United States of*  
501 *America*, 116(19), 9285–9292. <https://doi.org/10.1073/pnas.1901600116>
- 502 Coughlan, G., Laczó, J., Hort, J., Minihane, A. M., & Hornberger, M. (2018, August 6).  
503 Spatial navigation deficits — Overlooked cognitive marker for preclinical Alzheimer  
504 disease? *Nature Reviews Neurology*, Vol. 14, pp. 496–506.  
505 <https://doi.org/10.1038/s41582-018-0031-x>
- 506 Crary, J. F., Trojanowski, J. Q., Schneider, J. A., Abisambra, J. F., Abner, E. L., Alafuzoff, I.,  
507 ... Nelson, P. T. (2014). Primary age-related tauopathy (PART): a common pathology  
508 associated with human aging. *Acta Neuropathologica*, 128(6), 755–766.  
509 <https://doi.org/10.1007/s00401-014-1349-0>
- 510 Dafni-Merom, A., Peters-Founshtein, G., Kahana-Merhavi, S., & Arzy, S. (2019). A unified  
511 brain system of orientation and its disruption in Alzheimer's disease. *Annals of Clinical*  
512 *and Translational Neurology*, 6(12), 2468–2478. <https://doi.org/10.1002/acn3.50940>
- 513 DeIpoli, A. R., Rankin, K. P., Mucke, L., Miller, B. L., Gorno-Tempini, M. L. (2007).  
514 Spatial cognition and the human navigation network in AD and MCI. *Neurology*, 69,  
515 986–997.
- 516 Du, M., Basyouni, R., & Parkinson, C. (2021). How does the brain navigate knowledge of  
517 social relations? Testing for shared neural mechanisms for shifting attention in space  
518 and social knowledge. *NeuroImage*, 235(March), 118019.  
519 <https://doi.org/10.1016/j.neuroimage.2021.118019>
- 520 Dubois, B., Slachevsky, a, Litvan, I., & Pillon, B. (2000). The FAB: a Frontal Assessment  
521 Battery at bedside. *Neurology*, 55(11), 1621–1626.  
522 <https://doi.org/10.1212/WNL.57.3.565>
- 523 El Haj, M., & Antoine, P. (2018). Context Memory in Alzheimer's Disease: The “who,  
524 Where, and When.” *Archives of Clinical Neuropsychology*, 33(2), 158–167.

- 525 <https://doi.org/10.1093/arclin/acx062>
- 526 Franzmeier, N., Dewenter, A., Frontzkowski, L., Dichgans, M., Rubinski, A., Neitzel, J., ...
- 527 Ewers, M. (2020). *Patient-centered connectivity-based prediction of tau pathology*
- 528 *spread in Alzheimer ' s disease*. (November).
- 529 Franzmeier, N., Neitzel, J., Rubinski, A., Smith, R., Strandberg, O., Ossenkoppele, R., ... Raj,
- 530 B. A. (2020). Functional brain architecture is associated with the rate of tau
- 531 accumulation in Alzheimer's disease. *Nature Communications*, *11*(1), 1–17.
- 532 <https://doi.org/10.1038/s41467-019-14159-1>
- 533 Fredericks, C. A., Sturm, V. E., Brown, J. A., Hua, A. Y., Bilgel, M., Wong, D. F., ... Seeley,
- 534 W. W. (2018). Early affective changes and increased connectivity in preclinical
- 535 Alzheimer's disease. *Alzheimer's and Dementia: Diagnosis, Assessment and Disease*
- 536 *Monitoring*, *10*, 471–479. <https://doi.org/10.1016/j.dadm.2018.06.002>
- 537 Gauthier, B., & van Wassenhove, V. (2016). Time is not space: Core computations and
- 538 domain-specific networks for mental travels. *Journal of Neuroscience*, *36*(47), 11891–
- 539 11903. <https://doi.org/10.1523/JNEUROSCI.1400-16.2016>
- 540 Gauthier, S., Reisberg, B., Zaudig, M., Petersen, R. C., Ritchie, K., Broich, K., ... Winblad,
- 541 B. (2006). Mild cognitive impairment. *Lancet (London, England)*, *367*(9518), 1262–
- 542 1270. [https://doi.org/10.1016/S0140-6736\(06\)68542-5](https://doi.org/10.1016/S0140-6736(06)68542-5)
- 543 Hachinski, V. C., Iliff, L. D., Zilhka, E., Du Boulay, G. H., McAllister, V. L., Marshall, J., ...
- 544 Symon, L. (1975). Cerebral blood flow in dementia. *Archives of Neurology*, *32*(9), 632–
- 545 637.
- 546 Hayman, M., & Arzy, S. (2021). Mental travel in the person domain. *Journal of*
- 547 *Neurophysiology*, *20*(7), 464–476. <https://doi.org/10.1152/jn.00695.2020>
- 548 Hoenig, M. C., Bischof, G. N., Seemiller, J., Hammes, J., Kukulja, J., Onur, Ö. A., ...
- 549 Drzezga, A. (2018). Networks of tau distribution in Alzheimer's disease. *Brain*, *141*(2),
- 550 568–581. <https://doi.org/10.1093/brain/awx353>

- 551 Huijbers, W., Mormino, E. C., Schultz, A. P., Wigman, S., Ward, A. M., Larvie, M., ...  
552 Sperling, R. A. (2015). Amyloid- $\beta$  deposition in mild cognitive impairment is associated  
553 with increased hippocampal activity, atrophy and clinical progression. *Brain*, *138*(4),  
554 1023–1035. <https://doi.org/10.1093/brain/awv007>
- 555 Kanda, T., Ishii, K., Uemura, T., Miyamoto, N., Yoshikawa, T., Kono, A. K., & Mori, E.  
556 (2008). Comparison of grey matter and metabolic reductions in frontotemporal dementia  
557 using FDG-PET and voxel-based morphometric MR studies. *European Journal of*  
558 *Nuclear Medicine and Molecular Imaging*, *35*(12), 2227–2234.  
559 <https://doi.org/10.1007/s00259-008-0871-5>
- 560 Kaplan, R., & Friston, K. J. (2018). Hippocampal-entorhinal transformations in abstract  
561 frames of reference. *Entorhinal Transformations in Abstract Frames of Reference*,  
562 414524. <https://doi.org/10.1101/414524>
- 563 Kern, S., Zetterberg, H., Kern, J., Zettergren, A., Waern, M., Höglund, K., ... Skoog, I.  
564 (2018). Prevalence of preclinical Alzheimer disease: Comparison of current  
565 classification systems. *Neurology*, *90*(19), E1682–E1691.  
566 <https://doi.org/10.1212/WNL.0000000000005476>
- 567 Kumaran, D., & Maguire, E. A. (2005). The human hippocampus: Cognitive maps or  
568 relational memory? *Journal of Neuroscience*, *25*(31), 7254–7259.  
569 <https://doi.org/10.1523/JNEUROSCI.1103-05.2005>
- 570 Kunz, L., Schröder, T. N., Lee, H., Montag, C., Lachmann, B., Sariyska, R., ... Axmacher, N.  
571 (2015). Reduced grid-cell-like representations in adults at genetic risk for Alzheimer's  
572 disease. *Science (New York, N.Y.)*, *350*(6259), 430–433.  
573 <https://doi.org/10.1126/science.aac8128>
- 574 Lin, C., Ly, M., Karim, H. T., Wei, W., Snitz, B. E., Klunk, W. E., & Aizenstein, H. J. (2020).  
575 The effect of amyloid deposition on longitudinal resting-state functional connectivity in  
576 cognitively normal older adults. *Alzheimer's Research and Therapy*, *12*(1), 1–10.

- 577 <https://doi.org/10.1186/s13195-019-0573-1>
- 578 Mathuranath, P. S., Nestor, P. J., Berrios, G. E., Rakowicz, W., & Hodges, J. R. (2000). A  
579 brief cognitive test battery to differentiate Alzheimer’s disease and frontotemporal  
580 dementia. *Neurology*, 55(11), 1613–1620. Retrieved from  
581 <http://www.ncbi.nlm.nih.gov/pubmed/11113213>
- 582 Mckhann, G., Drachman, D., Folstein, M., Katzman, R., Price, D., & Stadlan, E. M. (n.d.).  
583 *Clinical diagnosis of Alzheimer’s disease: Task Force on Alzheimer’s Disease*.
- 584 Morris, J. C. (1993). The Clinical Dementia Rating (CDR): current version and scoring rules.  
585 *Neurology*, 43(11), 2412–2414. <https://doi.org/10.1212/WNL.43.11.2412-a>
- 586 Nasreddine, Z., Phillips, N., Bédirian, V., Charbonneau, S., Whitehead, V., Collin, I., ...  
587 Chertkow, H. (2005). The Montreal Cognitive Assessment, MoCA: a brief screening  
588 tool for mild cognitive impairment. *Journal of the American Geriatrics Society*, 53(4),  
589 695–699. <https://doi.org/10.1111/j.1532-5415.2005.53221.x>
- 590 Omer, D. B., Maimon, S. R., Las, L., & Ulanovsky, N. (2018). Social place-cells in the bat  
591 hippocampus. *Science*, 359(6372), 218–224. <https://doi.org/10.1126/science.aao3474>
- 592 Palmqvist, S., Schöll, M., Strandberg, O., Mattsson, N., Stomrud, E., Zetterberg, H., ...  
593 Hansson, O. (2017). Earliest accumulation of  $\beta$ -amyloid occurs within the default-mode  
594 network and concurrently affects brain connectivity. *Nature Communications*, 8(1).  
595 <https://doi.org/10.1038/s41467-017-01150-x>
- 596 Park, S. A., Miller, D. S., & Boorman, E. D. (2021). Inferences on a multidimensional social  
597 hierarchy use a grid-like code. *Nature Neuroscience*, 24(9), 1292–1301.  
598 <https://doi.org/10.1038/s41593-021-00916-3>
- 599 Parkinson, C., Liu, S., & Wheatley, T. (2014). A common cortical metric for spatial,  
600 temporal, and social distance. *The Journal of Neuroscience*, 34(5), 1979–1987.  
601 <https://doi.org/10.1523/JNEUROSCI.2159-13.2014>
- 602 Peer, M., Lyon, R., & Arzy, S. (2014). Orientation and disorientation: Lessons from patients

- 603 with epilepsy. *Epilepsy and Behavior*, *41*, 149–157.
- 604 <https://doi.org/10.1016/j.yebeh.2014.09.055>
- 605 Peer, M., Salomon, R., Goldberg, I., Blanke, O., & Arzy, S. (2015). Brain system for mental  
606 orientation in space, time, and person. *Proceedings of the National Academy of*  
607 *Sciences*, *112*(35), 11072–11077. <https://doi.org/10.1073/pnas.1504242112>
- 608 Peters-Founshtein, G., Peer, M., Rein, Y., Kahana Merhavi, S., Meiner, Z., & Arzy, S. (2018).  
609 Mental-orientation: A new approach to assessing patients across the Alzheimer’s disease  
610 spectrum. *Neuropsychology*. <https://doi.org/10.1037/neu0000463>
- 611 Peters-founshtein, G., Peer, M., Rein, Y., Merhavi, S. K., Meiner, Z., Peters-founshtein, G.,  
612 ... Meiner, Z. (2018). Mental-orientation: A new approach to assessing patients across  
613 the Alzheimer’s disease spectrum. *Neuropsychology*.
- 614 Petersen, R. C., Smith, G. E., Waring, S. C., Ivnik, R. J., Tangalos, E. G., & Kokmen, E.  
615 (1999). Mild Cognitive Impairment. *Archives of Neurology*, *56*(3), 303.  
616 <https://doi.org/10.1001/archneur.56.3.303>
- 617 Sabat, S. R., & Gladstone, C. M. (2010). What intact social cognition and social behavior  
618 reveal about cognition in the moderate stage of Alzheimer’s disease: A case study.  
619 *Dementia*, *9*(1), 61–78. <https://doi.org/10.1177/1471301210364450>
- 620 Sabat, S. R., & Lee, J. M. (2012). Relatedness among people diagnosed with dementia: Social  
621 cognition and the possibility of friendship. *Dementia*, *11*(3), 315–327.  
622 <https://doi.org/10.1177/1471301211421069>
- 623 Schaefer, A., Kong, R., Gordon, E. M., Laumann, T. O., Zuo, X.-N., Holmes, A. J., ... Yeo,  
624 B. T. T. (2018). Local-Global Parcellation of the Human Cerebral Cortex from Intrinsic  
625 Functional Connectivity MRI. *Cerebral Cortex*, *28*(9), 3095–3114.  
626 <https://doi.org/10.1093/cercor/bhx179>
- 627 Schafer, M., & Schiller, D. (2018). Navigating Social Space. *Neuron*, *100*(2), 476–489.  
628 <https://doi.org/10.1016/j.neuron.2018.10.006>



- 629 Silson, E. H., Steel, A., Kidder, A., Gilmore, A. W., & Baker, C. I. (2019). Distinct  
630 subdivisions of human medial parietal cortex support recollection of people and places.  
631 *ELife*, 1–25. <https://doi.org/10.1101/554915>
- 632 Sturm, V. E., Yokoyama, J. S., Seeley, W. W., Kramer, J. H., Miller, B. L., & Rankin, K. P.  
633 (2013). Heightened emotional contagion in mild cognitive impairment and Alzheimer’s  
634 disease is associated with temporal lobe degeneration. *Proceedings of the National*  
635 *Academy of Sciences of the United States of America*, 110(24), 9944–9949.  
636 <https://doi.org/10.1073/pnas.1301119110>
- 637 Townsend, J. T., & Ashby, F. G. (1983). Stochastic Modeling of Elementary Psychological  
638 Processes. *The American Journal of Psychology*, 480. <https://doi.org/10.2307/1422636>
- 639 van der Kant, R., Goldstein, L. S. B., & Ossenkoppele, R. (2020). Amyloid- $\beta$ -independent  
640 regulators of tau pathology in Alzheimer disease. *Nature Reviews Neuroscience*, Vol.  
641 21, pp. 21–35. <https://doi.org/10.1038/s41583-019-0240-3>
- 642 Whittington, J. C. R., McCaffary, D., Bakermans, J. J. W., & Behrens, T. E. J. (2022). How to  
643 build a cognitive map. *Nature Neuroscience*, 25(10), 1257–1272.  
644 <https://doi.org/10.1038/s41593-022-01153-y>
- 645 Whittington, J. C. R., Muller, T. H., Mark, S., Chen, G., Barry, C., Burgess, N., & Behrens, T.  
646 E. J. (2020). The Tolman-Eichenbaum Machine: Unifying Space and Relational  
647 Memory through Generalization in the Hippocampal Formation. *Cell*, 183(5), 1249-  
648 1263.e23. <https://doi.org/10.1016/j.cell.2020.10.024>
- 649 Wilson, R. S., Krueger, K. R., Arnold, S. E., Schneider, J. A., Kelly, J. F., Barnes, L. L., ...  
650 Bennett, D. A. (2007). Loneliness and risk of Alzheimer disease. *Archives of General*  
651 *Psychiatry*, 64(2), 234–240. <https://doi.org/10.1001/archpsyc.64.2.234>
- 652 Worsley, K. J., & Friston, K. J. (1995). Analysis of fMRI time-series revisited — Again.  
653 *NeuroImage*, 2(3), 173–181. <https://doi.org/10.1006/nimg.1995.1023>
- 654

655 **Table 1 – Demographics and neuropsychological assessment scores**

	CN	MCI	AD dementia
Gender (F   M)	9   7	14   9	4   8
Age (years)	69.5 ± 1.2	73.13 ± 1.38	70.75 ± 1.91
Education (years)	17.31 ± 0.8	16.45 ± 1	14.5 ± 1.31
MMSE <sup>a,b,c</sup>	29 ± 0.24	26.72 ± 0.46	21.86 ± 1.1
ACE <sup>a,b,c</sup>	94.78 ± 1	85.71 ± 1.61	66.46 ± 3.9
MoCA <sup>a,b,c</sup>	28.63 ± 0.38	24.72 ± 0.52	18.5 ± 1.33
CDR global <sup>a,b,c</sup>	0.21 ± 0.06	0.57 ± 0.05	1.17 ± 0.19

656

657 MMSE – Mini-mental state examination, ACE – Addenbrooke's cognitive examination,

658 MoCA – Montreal cognitive assessment, CDR – clinical dementia rating

659 <sup>a</sup> Statistically significance (p<.05) between CN and AD dementia

660 <sup>b</sup> Statistically significance (p<.05) between CN and MCI

661 <sup>c</sup> Statistically significance (p<.05) between CN and MCI

662

663

664

665

666

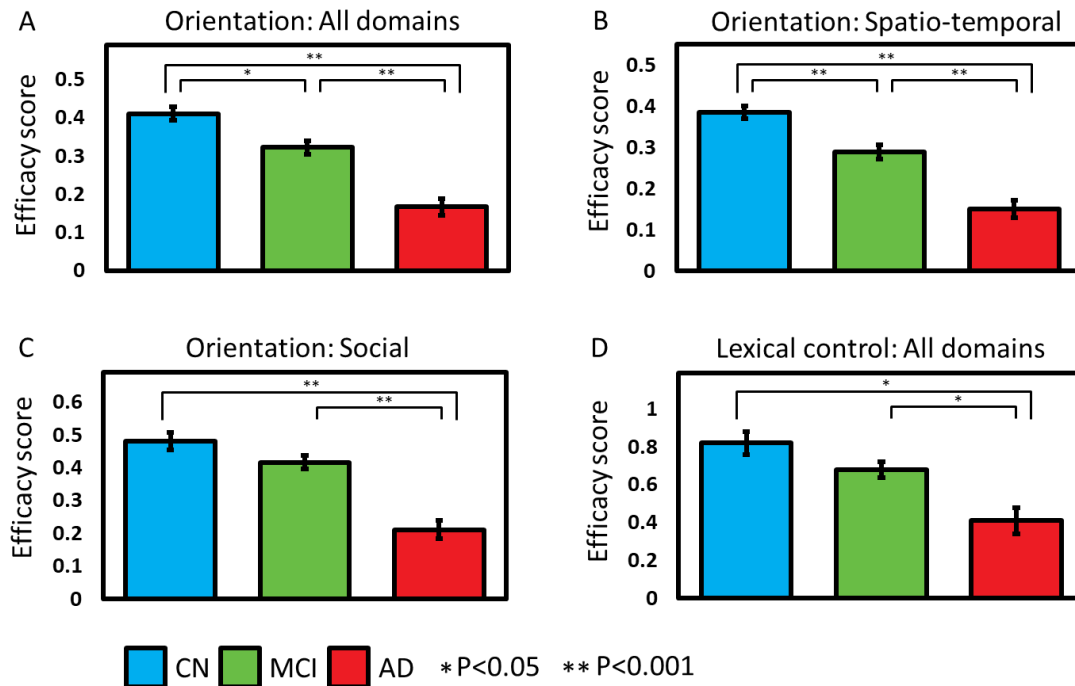
667

668

669

670

## Spatio-temporal and social orientation changes in AD



671

672 **Figure 1. Spatio-temporal and social orientation changes along the AD continuum.** Mean

673 efficacy scores (ES) of CN (N= 16, blue), MCI (N = 23, green) and AD dementia participants

674 (N = 12, red) for the orientation task in all domains (A), the orientation task in the domains of

675 space and time (spatio-temporal) (B), the orientation task in person (social) (C), and the lexical

676 control task in all domains (D). Significant CN-MCI differences were found in all domain

677 orientation (A;  $P < 0.05$ ), and space and time orientation (B;  $P < 0.001$ ). Significant MCI-AD

678 dementia and CN-AD dementia differences were found in all domains, spatio-temporal and

679 social orientation task ES (A, B, C;  $P < 0.001$ ), as well as in the lexical task (D;  $P < 0.05$ ).

680 Statistical significance was estimated using ANOVA and Tukey-Kramer post hoc test.

681

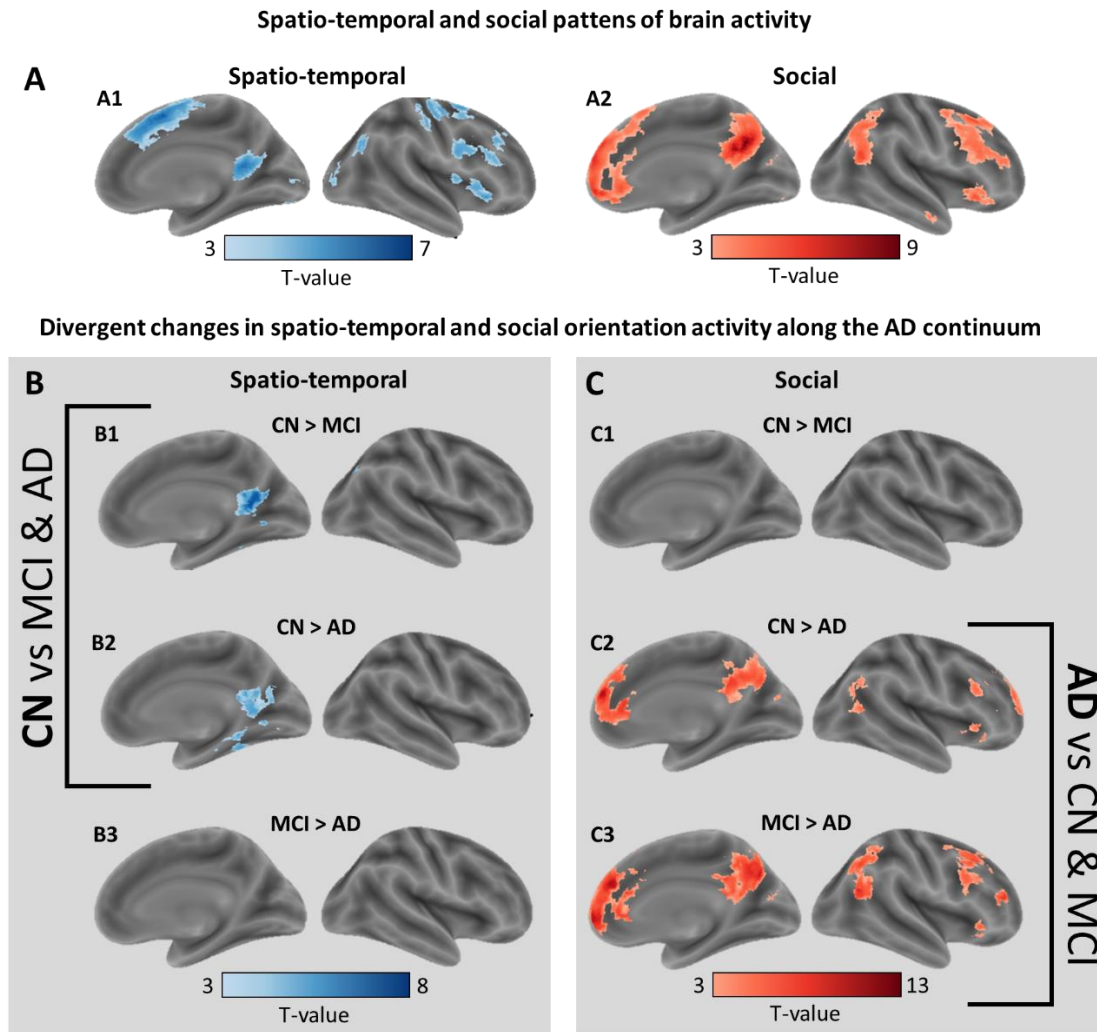
682

683

684

685

## Changes in spatio-temporal and social orientation activity in AD



686

687 **Figure 2. Changes in spatio-temporal and social orientation activity in AD.** (A) Spatio-  
688 temporal and social patterns of brain activity. Results of GLM analysis exhibiting contrast maps  
689 of spatio-temporal (A1) and social (A2) orientation tasks over the lexical control task (All  
690 participants,  $DF=50$ ,  $P<0.05$  FDR corrected, cluster size  $> 20$  voxels). (B, C) Divergent changes  
691 in spatio-temporal and social orientation activity. Spatio-temporal (B) and social (C)  
692 disorientation contrasted task-evoked activity maps across the three clinical groups: CN greater  
693 than MCI participants in spatio-temporal (B1) and social (C1) orientation ( $DF=38$ ,  $P<0.05$  FDR  
694 corrected, cluster size thresholding of 20 voxels); CN greater than AD dementia participants in  
695 spatio-temporal (B2) and social (C2) orientation ( $DF=34$ ,  $P<0.05$  FDR corrected, cluster size

696 thresholding of 20 voxels); MCI greater than AD dementia participants in spatio-temporal (B3)  
697 and social (C3) orientation (DF=27,  $P < 0.05$  FDR corrected, cluster size thresholding of 20  
698 voxels).

699

700

701

702

703

704

705

706

707

708

709

710

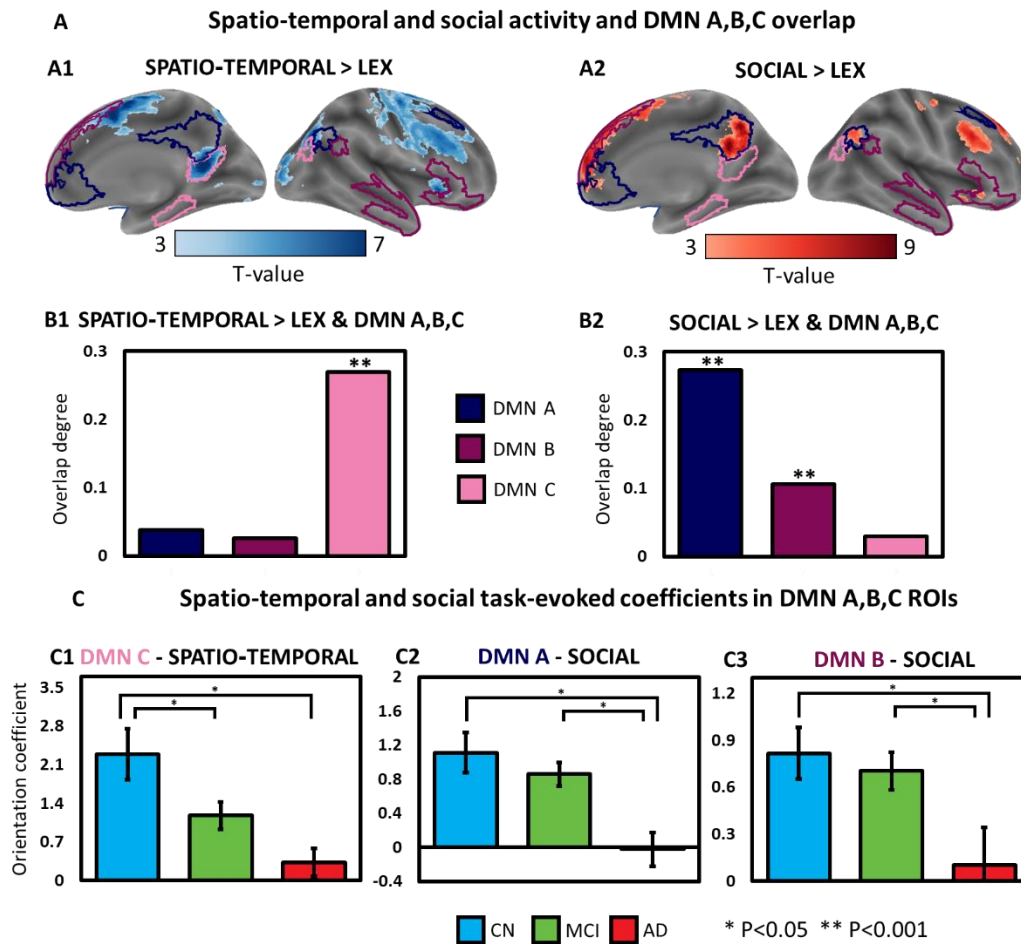
711

712

713

714

## Orientation-evoked activity overlaps Default Mode sub-networks



715

716 **Figure 3. Orientation-evoked activity overlaps Default Mode sub-networks differently.**

717 (A) Spatio-temporal and social activity and DMN A, B, and C overlap. Delineations of DMN

718 sub-networks (Schaefer et. al, 2018) DMN A (dark), DMN B (medium), DMN C (light)

719 superimposed on maps of spatio-temporal (A1) and social (A2) orientation tasks (Orientation

720 > Lexical control; All participants, DF=50, P<0.05 FDR corrected, cluster size > 20 voxels).

721 (B) The percent of overlap between supra-threshold task-evoked spatio-temporal (B1) and

722 social (B2) maps and DMN subnetworks A, B, and C. Asterisks indicate significant overlap

723 (permutation test, 10,000 iterations). (C) Spatio-temporal and social task-evoked coefficients

724 in DMN A, B, and C ROIs. Mean GLM-derived parameter estimates for social (C2 and 3) and

725 spatio-temporal (C1) orientation (>rest) in significantly overlapping (B) DMN subnetworks (C1

726 – DMN C - spatio-temporal; C2 –DMN B – social; C3 – DMN C - social) for CN (N= 16, blue),  
727 MCI (N = 23, green) and AD dementia (N = 12, red). Significant differences were found  
728 between CN and AD dementia participants in DMN A, B, and C, between MCI and AD  
729 dementia participants in DMN A and B, and between CN and MCI participants in DMN C  
730 (ANOVA and Tukey-Kramer post hoc test,  $P < 0.05$ ).

731

732

733

734

735

736

737

738

739

740

741

742

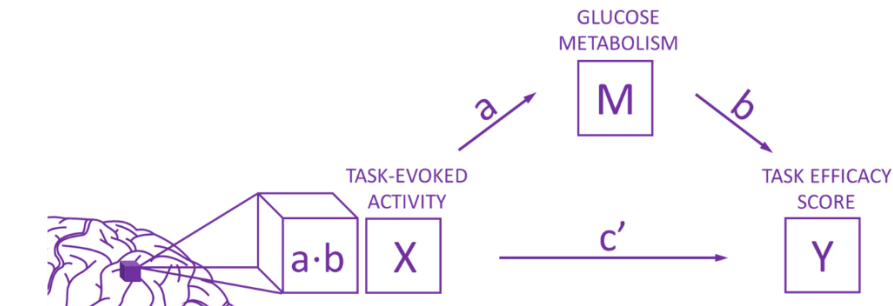
743

744

745

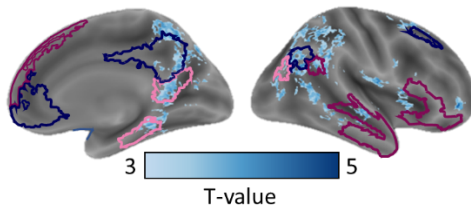
## Mediation models of brain activity, glucose metabolism and orientation performance

### A Schematic of mediation model of brain activity, glucose metabolism and orientation performance

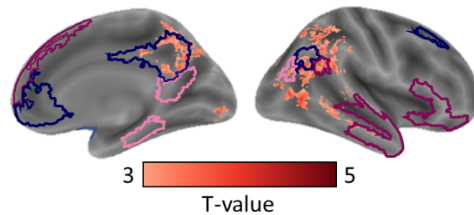


### B Spatio-temporal and social activity and DMN A,B,C overlap

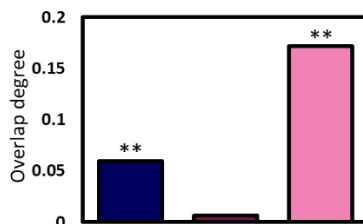
#### B1 MEDIATION: SPATIO-TEMPORAL



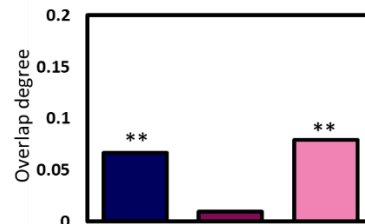
#### B2 MEDIATION: SOCIAL



#### C1 SPATIO-TEMPORAL MEDIATION & DMN A,B,C



#### C2 SOCIAL MEDIATION & DMN A,B,C



746

747 **Figure 4. Mediation models of brain activity, glucose metabolism and orientation**

748 **performance.** (A) Mediation analysis was used to test the hypothesis that changes in FDG-

749 PET uptake (M) across the AD continuum alter the relations between spatio-temporal (B1) and

750 social (B2) orientation-evoked brain activity (X) and orientation task performance (Y). (B)

751 Spatio-temporal and social mediation and DMN A, B, and C overlap. Delineations of DMN

752 sub-networks (Schaefer et. al, 2018) DMN A (dark), DMN B (medium), and DMN C (light)

753 superimposed on maps of spatio-temporal (B1) and social (B2) mediation ( $P < 0.05$ , FDR-

754 corrected). (C) The percent of overlap between supra-threshold task-evoked spatio-temporal

755 (C1) and social (C2) suprathreshold mediation maps and DMN subnetworks A, B, and C.

756 Asterisks indicate significant overlap (permutation test, 10,000 iterations).